The Journal of Infectious Diseases

MAJOR ARTICLE

Functional Human CD141$^+$ Dendritic Cells in Human Immune System Mice

Jordana G. A. Coelho-dos-Reis,[1,2] Ryota Funakoshi,[1,a] Jing Huang,[1] Felipe Valença Pereira,[1,3] Sho Iketani,[1,4] and Moriya Tsuji[1]

[1]Aaron Diamond AIDS Research Center, Affiliate of The Rockefeller University, New York, New York, USA, [2]Department of Microbiology, Universidade Federal de Minas Gerais, Minas Gerais, Brazil, [3]Federal University of Sao Paulo, Sao Paulo, Brazil, [4]Department of Microbiology and Immunology, Columbia University Irving Medical Center, New York, New York, USA

Background. For the purpose of studying functional human dendritic cells (DCs) in a humanized mouse model that mimics the human immune system (HIS), a model referred to as HIS mice was established.

Methods. Human immune system mice were made by engrafting NOD/SCID/IL2Rgamma^{null} (NSG) mice with human hematopoietic stem cells (HSCs) following the transduction of genes encoding human cytokines and human leukocyte antigen (HLA)-A2.1 by adeno-associated virus serotype 9 (AAV9) vectors.

Results. Our results indicate that human DC subsets, such as CD141$^+$CD11c$^+$ and CD1c$^+$CD11c$^+$ myeloid DCs, distribute throughout several organs in HIS mice including blood, bone marrow, spleen, and draining lymph nodes. The CD141$^+$CD11c$^+$ and CD1c$^+$CD11c$^+$ human DCs isolated from HIS mice immunized with adenoviruses expressing malaria/human immunodeficiency virus (HIV) epitopes were able to induce the proliferation of malaria/HIV epitopes-specific human CD8$^+$ T cells in vitro. Upregulation of CD1c was also observed in human CD141$^+$ DCs 1 day after immunization with the adenovirus-based vaccines.

Conclusions. Establishment of such a humanized mouse model that mounts functional human DCs enables preclinical assessment of the immunogenicity of human vaccines in vivo.

Keywords. adenovirus vaccine; CD141; CD1c; human dendritic cells; human immune system mice.

Dendritic cells (DCs) have been one of the most well studied subsets of antigen-presenting cells (APCs) since their discovery [1–4]. The myeloid lineage is responsible for originating classic DCs (cDCs) or myeloid DCs (mDCs), whereas the lymphoid lineage originates plasmacytoid DCs (pDCs) [5–6]. Human mDCs can express either surface molecules such as CD141, a cofactor to thrombin that also regulates complement components, and CD1c, a central molecule DCs utilize to present lipid antigens [7, 8]. Coexpression of CD141 and CD1c has been rarely found on DCs in steady-state or short-term culture [7], but it is found in some barrier tissues, such as cutaneous and mucosal tissues [9–11]. Prior functional in vivo studies on human CD141$^+$CD11c$^+$ and CD1c$^+$CD11c$^+$ DCs to define their specific contribution to antigen presentation have been hindered by 3 obstacles: (1) the low frequency of these DCs in human blood, (2) the difficulties in studying human tissues, and (3) the discrepancies between murine and human DCs [12–14]. Such functional studies are essential for defining the role and characterization of DC subsets that are capable of inducing robust activation and proliferation of CD8$^+$ T cells [15–17].

One strategy to overcome such obstacles is the optimized reconstitution of the human immune system (HIS) in highly immunodeficient mice, such as NOD/SCID/IL2Rgamma^{null} (NSG) mice. This strategy involves the use of transgenic or knock-in mice expressing human genes, or the surgical transplantation of human thymus/liver to NSG mice [10, 18–22]. However, the production of artificial levels of human cytokines and the large degree of mouse-to-mouse variability with regards to the HIS reconstitution have posed a challenge to study the phenotypes and function of DCs in blood and tissues of humanized mice [23]. Therefore, in this study, a unique way of making NSG mice that possess the HIS was used by way of adeno-associated virus (AAV)-based gene delivery [24, 25]. We have previously shown that injection of NSG mice with recombinant AAV serotype 9 (rAAV9) vectors that encode human leukocyte antigen (HLA)-A2.1 and human hematopoietic cytokines facilitated more than 80% reconstitution of tissue and circulating human CD45$^+$ leukocytes [26, 27]. In this study, using rAAV9 vectors that encode human hematopoietic cytokines that are crucial for the development and differentiation of various immunocompetent cells, we could phenotypically characterize human DCs, in particular, human CD141$^+$CD11c$^+$ and CD1c$^+$CD11c$^+$ DCs, in a humanized mouse model.

Received 12 December 2018; editorial decision 12 August 2019; accepted 20 August 2019; published online October 25, 2019.

[a]This article is dedicated to the memory of our beloved friend and amazing colleague, Ryota Funakoshi, who recently passed away. He is deeply missed by all of us.

Presented in part: Keystone Symposia, Advancing Vaccines in The Genomic Era, 31 October–4 November 2013, Rio de Janeiro, Brazil.

Correspondence: Moriya Tsuji, MD, PhD, Aaron Diamond AIDS Research Center, 455 First Ave Room 747, New York, NY 10016 (mtsuji@adarc.org).

The Journal of Infectious Diseases® 2020;221:201–13

© The Author(s) 2019. Published by Oxford University Press for the Infectious Diseases Society of America. All rights reserved. For permissions, e-mail: journals.permissions@oup.com.

DOI: 10.1093/infdis/jiz432

MATERIAL AND METHODS

Mice

NOD.Cg-Prkdc^{scid} IL2Rg^{tmWjl}/Sz (NSG) mice were purchased from The Jackson Laboratories. The NSG mice were maintained under pathogen-free conditions in the animal facility at the Comparative Bioscience Center of The Rockefeller University.

Generation of Adeno-Associated Virus Vectors

The rAAV9 vectors that express genes that encode human hematopoietic cytokines (granulocyte-macrophage colony-stimulating factor [GM-CSF], interleukin [IL]-3, and IL-15) and HLA-A2.1 were prepared as previously described [26]. The viral titer and transgene expression levels were also determined as described [26, 27].

Purification and Infusion of Human Hematopoietic Stem Cells

Human CD34$^+$ hematopoietic stem cells (HSCs) were purified from mononuclear cells isolated from fetal liver tissues using antihuman CD34$^+$ microbeads (Miltenyi Biotec, Cologne, Germany), and the percentage of CD34$^+$ cells was confirmed to be higher than 90% by flow cytometry. Two-week-old NSG mice were first given injections with rAAV9 vectors that encode human cytokines (hucytokines), ie, IL-3, IL-15, and GM-CSF, as well as HLA-A2.1. Because AAV9 that encodes human GM-CSF (AAV9/GM-CSF) was essential for reconstitution of human cells in previous studies, 1×10^8, 1×10^9, and 5×10^9 genomic copies of this AAV9 were given to NSG mice in the titration experiments. Combined rAAV9 treatments had 5×10^9 genomic copies of each AAV9 that encodes the cytokines IL-3 and IL-15. For AAV9 that encodes HLA-A2.1 (AAV9/A2), 5×10^{10} genomic copies were given to mice by perithoracic injection and 5×10^{10} genomic copies by intravenous injection. Two weeks after transduction, myeloablation was induced by 150 cGy total body sublethal irradiation, and, on the next day, each A2/hucytokines-transduced, irradiated NSG mouse was given intravenous injection with 1×10^5 human HSCs.

Phenotypic Analyses of Human Lymphocytes and Dendritic Cells in the Blood of Human Immune System Mice

Human CD45$^+$ leukocytes and DC subsets were monitored in the bone marrow (BM), spleen, and blood of A2/hucytokines-transduced NSG mice after the human HSC infusion by flow cytometric analysis. Human immune cells from blood were evaluated 6, 10, and 14 weeks after HSC infusion, whereas cells from the BM and spleen were evaluated 18 weeks after HSC infusion [26]. Cells were washed and stained for 40 minutes on ice in the dark with the following antibodies purchased from BioLegend: Pacific Blue antihuman CD45 (clone HI30), PerCP/Cy5.5 antimouse CD45 (clone 30-F11), phycoerythrin (PE)-Cy7 antihuman CD141 (clone M80), APC-Cy7 antihuman CD1c (clone L161), fluorescein isothiocyanate (FITC) antihuman Lin (CD3, CD14, CD16, and CD19; clones UCHT1, HCD14, 3G8, and HIB19, respectively), PE antihuman CD11c (clone Bu15), Alexa Fluor 647 antihuman CD86 (clone IT2.2), Alexa Fluor 700 anti-HLA-DR (clone LN3), and APC anti-HLA-ABC (clone W6/32). After staining, cells were washed twice with phosphate-buffered saline containing 2% fetal bovine serum, fixed with 1% paraformaldehyde, and analyzed using a BD LSR II (BD Biosciences, San Jose, CA).

Immunization of Human Immune System Mice With Recombinant Adenovirus Vaccines That Express Malaria/Human Immunodeficiency Virus Antigens

After confirming the successful establishment (the percentage of human CD45$^+$ cells among human and mouse CD45$^+$ cells combined in peripheral blood mononuclear cells [PBMCs] was >80%) of HIS in A2/hucytokines-transduced NSG mice 18 weeks after HSC infusion, immunizations were conducted. As a model of vaccination, high or low doses of a recombinant adenovirus serotype 5 (rAd5) that expresses the *Plasmodium falciparum* circumsporozoite protein (AdPfCS) or the p24 antigen of HIV-1 (Adp24) were used [26]. The HIS mice were immunized intramuscularly with high (5×10^{10} viral particle units [vpu]) or low (5×10^7 vpu) doses of each AdPfCS and Adp24. Subsets of DCs were monitored before, and 1 and 4 days after, immunization.

In Vitro Stimulation of Vaccine-Induced Human CD8$^+$ T Cells by Dendritic Cells

For the in vitro proliferation assay, splenic CD8$^+$ T cells were isolated from HIS mice 15 days postimmunization with AdPfCS and Adp24 by negative selection (Stem Cell Technologies, Vancouver, Canada). CD8$^+$ T cells were then labeled with 6 μM carboxyfluorescein diacetate succinimidyl ester ([CFSE] Molecular Probes, Eugene, OR). Autologous DCs were used as APCs, prepared either from the BM or the lymph nodes (LNs) of AdPfCS/Adp24-immunized HIS mice. The BMs were harvested 15 days postvaccination, and LNs were harvested 12 or 24 hours postvaccination from different groups of mice. All groups of mice (for obtaining BM as well as 12- and 24-hour LNs) received HSCs from the same donor. For preparation of CD11c$^+$ DCs from BM, BM-derived DCs (BM-DCs) were obtained by culturing BM cells in the presence of human GM-CSF + human IL-4 for 5 days, washing, then resting for 24 hours in the absence of cytokines. Dendritic cells having specific surface markers were purified with further selection. The first round of purification was performed using the EasySep Human Myeloid DC Enrichment Kit (Stem Cell Technologies, Vancouver, Canada). Subsequently, the cells were incubated with FITC antihuman CD141 (clone M80) and PE antihuman CD1c (clone 161) antibodies, followed by selection using anti-FITC and anti-PE MACS beads (Miltenyi Biotec, Cologne, Germany). CD141$^+$CD1c$^-$ cells were isolated from this population by gating on the PE antihuman CD1c antibody signal.

For preparing LN-resident DCs, LNs from mice 12 and 24 hours after immunization with AdPfCS and Adp24 were harvested and a cell suspension was obtained, from which LN-resident $CD11c^+$ DCs were isolated using the EasySep Human Myeloid DC Enrichment Kit described above.

Dendritic cells were then pulsed with peptides corresponding to the HLA-A2-restricted $CD8^+$ T-cell epitopes of the PfCS protein (YLNKIQNSL; KLRKPKHKKL; SLKKNSRSL) [26] and HIV-p24 antigen (TLNAWVKVV) [26] at 20 μg/mL for 1 hour. The CFSE-labeled enriched $CD8^+$ T cells from AdPfCS/Adp24-immunized HIS mice were cocultured with respective DCs in 48-well plates at a 1:1 ratio (Costar, Corning, NY) for 6 days at 37°C in 5% CO_2. Then, cells were fixed with 1% paraformaldehyde, followed by washing and incubation with antimouse CD16/CD32 blocking antibodies. After blocking, cells were incubated with Alexa Fluor 700 antihuman CD8 (clone HP-3G10; BioLegend) and APC antihuman CD3 (clone HIT3a; BioLegend), washed, fixed, and analyzed using a BD LSR II.

Statistical Analysis

To compare the levels of different groups of mice and parameters evaluated, one-way analysis of variance with Dunnet's posttest was performed for parametric data, and Mann-Whitney test was used for non-parametric data. All statistical analyses were performed using GraphPad Prism software version 5.0 (GraphPad Software, San Diego, CA). A value of $P < .05$ was considered statistically significant.

RESULTS

Transduction of Human Granulocyte-Macrophage Colony-Stimulating Factor by rAAV9 Improves the Reconstitution of Human Myeloid Dendritic Cells in Human Immune System Mice

In this study, we sought to use an AAV9-based gene delivery system to improve the reconstitution of HIS, in particular, human mDCs, in mice. The NSG mice first received an intravenous injection of rAAV9 vectors that encode human hematopoietic cytokines, ie, GM-CSF, IL-3, and IL-15, followed by sublethal irradiation and infusion with human HSCs.

Figure 1*A* depicts our experimental scheme for monitoring the percentages of $HLA\text{-}DR^+CD11c^+$ mDCs in NSG mice 6, 10, 14, and 18 weeks after human HSC infusion. As shown in Figure 1*B*, NSG mice that received rAAV9 expressing all 3 human hematopoietic cytokines—human GM-CSF, IL-3, and IL-15—designated as "hucytokines", possessed a higher percentage of DCs in blood at 14 and 18 weeks post-HSC infusion compared to that in NSG mice that received rAAV9 expressing IL-3, IL-15, or GFP alone. Furthermore, this percentage was comparable to that observed in human blood by 14 weeks post-HSC infusion. IL-3 and IL-15 delivered by rAAV9 increased the percentage of human $CD45^+$ leukocytes in BM but did not alter their percentage in spleen (Figure 1*C*). In addition, these cytokines did not alter the percentages of $HLA\text{-}DR^+CD11c^+$ DCs in either BM or spleen. In contrast, GM-CSF delivered by rAAV9 alone (rAAV9/GM-CSF) could facilitate the reconstitution of not only human $CD45^+$ leukocytes, but, more importantly, human $CD11c^+$ mDCs in the spleen and BM of HIS mice in a rAAV9/GM-CSF dose-dependent manner (Figure 1*C*). The levels of human $CD11c^+$ DCs stabilized 14 weeks after HSC infusion, similar to other subsets such as T and B cells as reported previously [26]. Transduction of HLA-A2 by rAAV9 along with genes encoding GM-CSF, IL-3, and IL-15 did not seem to affect the repopulation of mDCs or pDCs (Supplementary Figure 1); however, the expression of this gene in thymus is essential for generating functional $CD8^+$ T cells [26].

Repopulation of Myeloid and Lymphoid Dendritic Cell Subsets in the Blood and Tissues of Human Immune System Mice

We then determined the levels of repopulation of pDCs and mDCs in hucytokines-transduced NSG mice, which received the combination of AAV9 encoding for IL-3/IL-15 (5×10^9 genomic copies) and GM-CSF (1×10^9 genomic copies) 18 weeks posthuman HSC infusion (Figure 2*A*). Gating strategies for pDCs ($CD123^+CD304^+CD11c^-$) and the 2 subsets of mDCs, $CD141^+CD11c^+$ DCs and $CD1c^+CD11c^+$ DCs, are shown in Figure 2*B* and *C*. All DCs were gated within the low granularity lymphocytic subset and as HLA-DR positive. In the peripheral blood of HIS mice, we observed a similar percentage of $CD141^+$ DCs as among human PBMCs (Figure 2*C*). A comprehensive analysis of DC subpopulations in HIS mice indicated that these mice repopulate several subsets of human DCs in blood, BM, and spleen (Figure 2*D*).

Vaccinated HIS Mice Have Increased $HLA\text{-}DR^{LOW/INT}$ Myeloid $CD11c^+$ DCs in Spleen and Lymph Node as Well as $HLA\text{-}DR^{HIGH}$ $CD11c^+$ DCs in Blood

To study DC biology in HIS mice upon vaccination, A2/hucytokines-transduced HIS mice were vaccinated with AdPfCS/Adp24 18 weeks after human HSC infusion [26]. Peripheral blood, spleen, and LNs were then harvested to phenotype and characterize the primary DCs by FACS (Figure 3*A*). Dendritic cell subsets could be defined by HLA-DR expression, with both migratory ($HLA\text{-}DR^{HIGH}$) and resident ($HLA\text{-}DR^{INT}$) observed in all organs (Figure 3*B*) [14]. Vaccination induced an increase in $HLA\text{-}DR^{HIGH}CD11c^+$ DCs in the peripheral blood along with an expansion of $HLA\text{-}DR^{INT}CD11c^+$ DCs in spleen and LNs (Figure 3*B* and *C*). The altered human major histocompatibility complex (MHC)-II dynamics in mDCs suggest that mDC biology and responsiveness postvaccination developed appropriately in the HIS mice.

Augmented Human Peripheral Blood Dendritic Cell Numbers, Subtypes, and Activation One Day Postvaccination of Human Immune System Mice

The kinetics of phenotypic and activation markers on the myeloid $CD11c^+$DCs were assessed before and 1 and 4 days

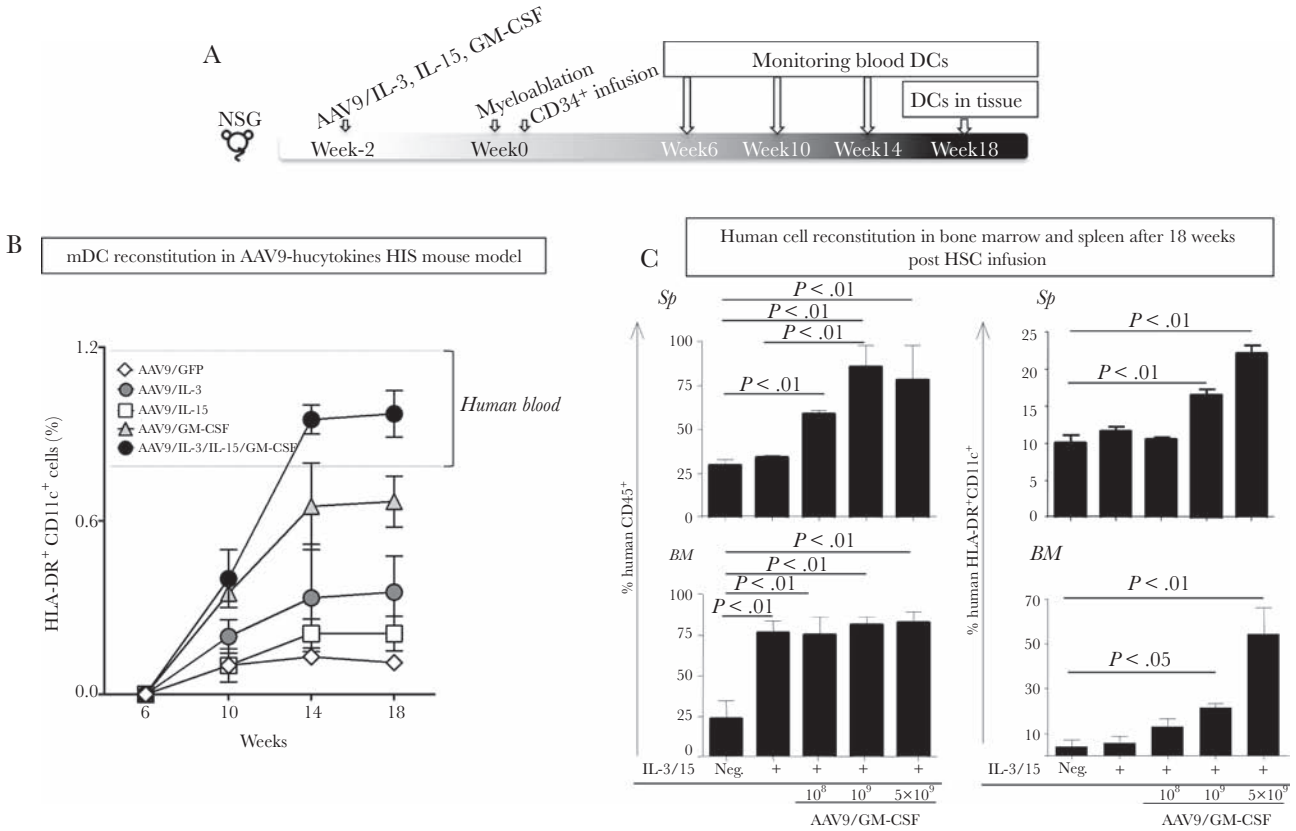

Figure 1. Reconstitution of human myeloid cells in human immune system (HIS) mice. (A) Experimental scheme to generate adeno-associated virus serotype 9 (AAV9)-hucytokines HIS mice. Recombinant AAV9 (rAAV9) vectors that encode human interleukin (IL)-3, IL-15, or granulocyte-macrophage colony-stimulating factor (GM-CSF) were administered separately, or in combination, to 2-week-old NOD/SCID/IL2Rgamma^{null} (NSG) mice. Recombinant rAAV9 encoding for green fluorescent protein was used as a mock control. Two weeks later, mice were sublethally irradiated for myeloablation, and 24 hours later, purified human CD34$^+$ hematopoietic stem cells (HSCs) were intravenously injected into mice. Reconstitution of human CD45$^+$ cells, as well as myeloid dendritic cells (mDCs), in blood and in tissues was monitored at 6, 10, 14, and 18 weeks post-HSC infusion. (B) For monitoring DCs, mouse CD45$^-$ human CD45$^+$ (mCD45$^-$hCD45$^+$) cells were gated on Lin$^-$ (CD3, CD14, CD16, and CD19) and evaluated for expression of human CD11c and human leukocyte antigen (HLA)-DR. The percentage of HLA-DR$^+$CD11c$^+$ DCs are displayed 6, 10, 14, and 18 weeks after the HSC infusion using line graphs with symbols representing the mean values and standard error lines. Dashed lines represent the minimum and maximum values for HLA-DR$^+$CD11c$^+$ DCs in human blood as reference for DC humanization. (C) Different doses, 10^8, 10^9, or 5×10^9 genomic copies, of rAAV9 that encodes 1 or all of human cytokines were injected into each NSG mouse, followed by HSC infusion. These mice were monitored for reconstitution of human CD45$^+$ cells, as well as HLA-DR$^+$CD11c$^+$ DCs in bone marrow (BM) and spleen. Experiments included 3–5 mice per group and were repeated 4 times. Results illustrate data from 1 representative experiment (n = 5). Statistical analyses were performed using analysis of variance followed by Dunnett's test and differences were considered if $P < .05$.

after vaccination with AdPfCS and Adp24 (Figure 4*A*). CD11c expression alone was not altered significantly by vaccination (data not shown). However, the percentages of HLA-DR$^+$CD11c$^+$ increased significantly 1 day after vaccination before returning to prevaccination baseline level by day 4 (Figure 4*B* and *C*). A similar trend was observed for the expression of CD86, CD141, and CD1c within HLA-DR$^+$CD11c$^+$ by fold-change analyses (Figure 4*D*).

Induction of Proliferation of Antigen-Specific CD8$^+$ T Cells From Vaccinated Human Immune System Mice by Human Myeloid Dendritic Cells

Our previous studies have shown that HIS mice transduced with AAV9/hucytokines and AAV9/A2 and infused with human HSCs possess functional HLA-A2-restricted human CD8$^+$ T cells [26]. Therefore, we sought to test whether human DC subsets identified in the current study could induce the proliferation of human CD8$^+$ T cells that were primed by rAd5-based vaccines. For this purpose, HIS mice were first immunized with 2 rAd5 vaccines, AdPfCS and Adp24 (Figure 5*A*) [26]. CD8$^+$ T cells were then collected from the spleen of HIS mice 15 days after immunization, CFSE labeled, and cocultured with autologous CD141$^+$ or CD1c$^+$ DCs isolated from BM-derived CD11c$^+$ DCs, as well as LN-derived CD11c$^+$ DCs, at a 1:1 ratio. All 3 long-term BM-derived DC subsets (total CD11c$^+$, CD141$^+$, and CD1c$^+$ DCs) from AAV9-A2/hucytokines-treated HIS mice induced the proliferation of CD8$^+$ T cells in vitro in an Ad vaccination dose-dependent manner (Figure 5*B* and *C*). Fold change analysis of proliferation index for peptide-loaded over unloaded DCs showed that APCs induced greatly increased proliferation in mice immunized with the high dose of vaccine (5×10^{10} vpu) compared with low dose (5×10^7 vpu). At the high dose of rAd5-vaccination, CD11c$^+$ DCs induced

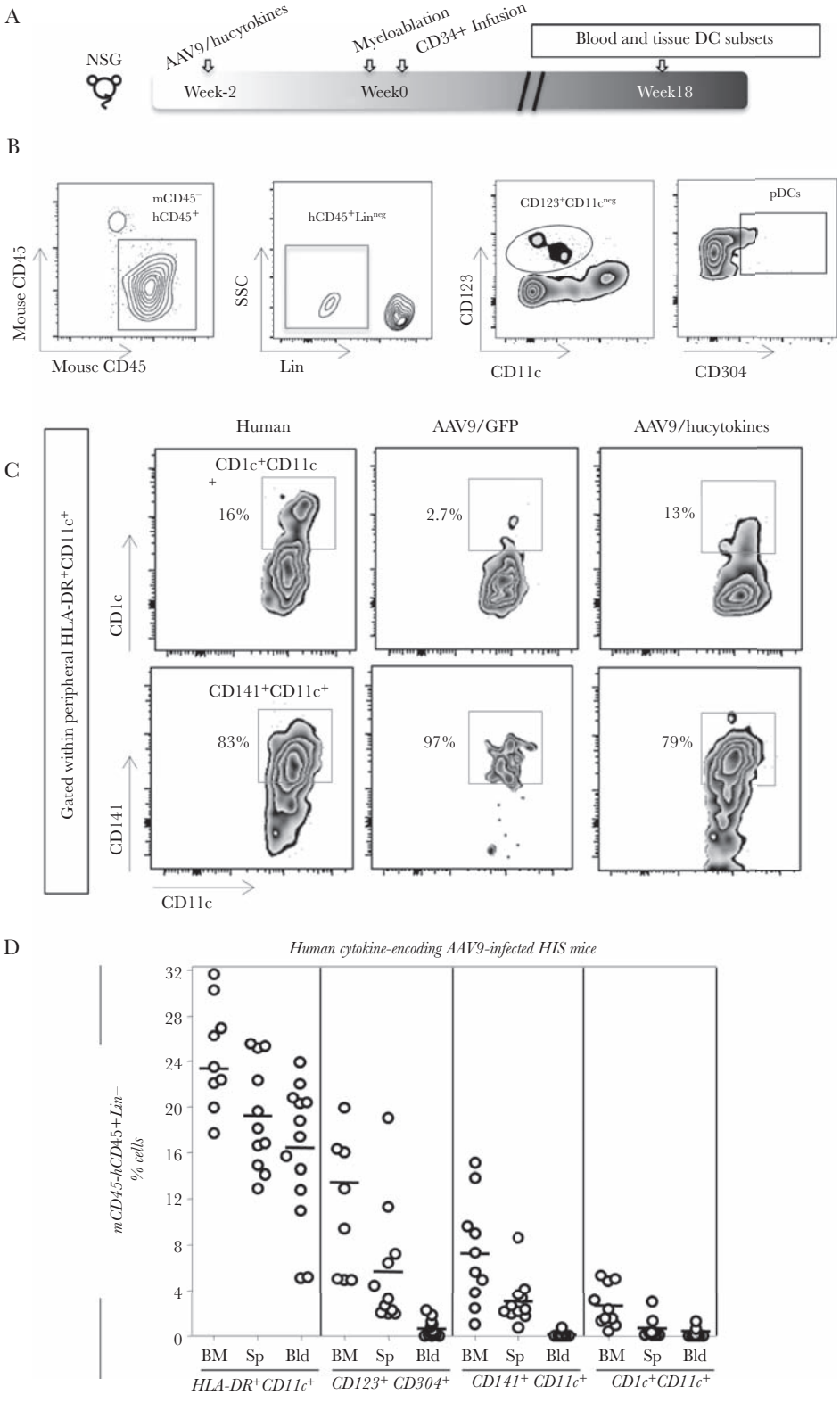

Figure 2. Emergence of myeloid and lymphoid dendritic cell (DC) subsets in blood and tissues of human immune system (HIS) mice. (A) The experimental scheme to generate HIS mice, similar to the one described in Figure 1A. (B) Gating strategy for defining plasmacytoid DCs (pDCs) ($CD304^+CD123^+CD11c^-$) are shown as density plots within peripheral human $mCD45^-hCD45^+Lin^-$ (the example shows a blood sample). (C) Zebra plots display the frequency of human leukocyte antigen (HLA)-DR^+CD11c^+ DC subsets that express either CD141 or CD1c versus CD11c among peripheral blood mononuclear cells collected from human or HIS mice. (D) Within the $mCD45^-CD45^+Lin^-$ population, the following phenotypic DC subsets, $HLA\text{-}DR^+CD11c^+$, $CD304^+CD123^+$, $CD141^+CD11c^+$, and $CD1c^+CD11c^+$, were evaluated in bone marrow (BM), spleen (Sp), and blood (Bld) of adeno-associated virus serotype 9 (AAV9)/hucytokines HIS mice. Experiments were repeated 4 times. NSG, NOD/SCID/IL2Rgamma^{null}; SSC, side scatter.

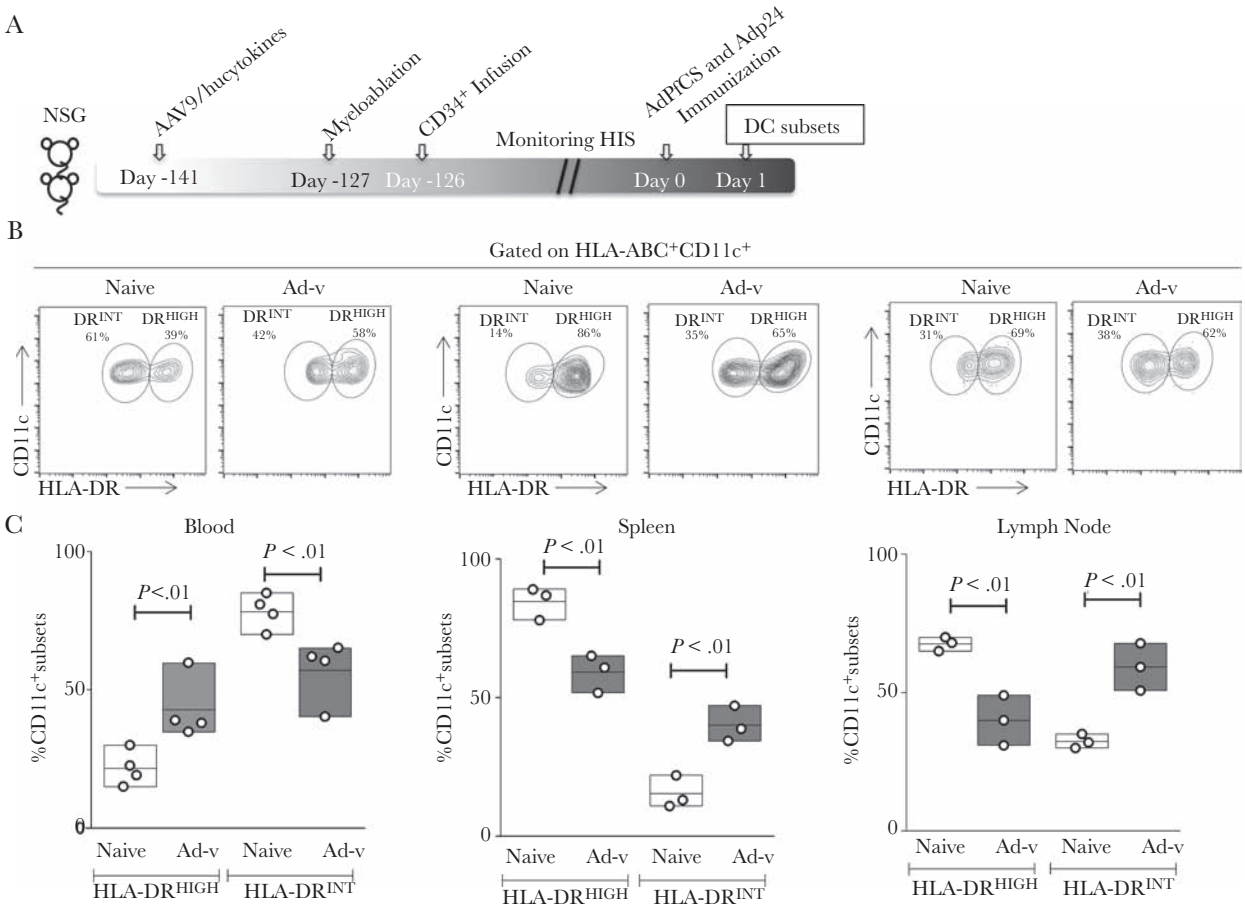

Figure 3. Defining resident human leukocyte antigen (HLA)-DR^{INT}CD11c^{+} dendritic cells (DCs) in spleen and lymph nodes (LNs) as well as migratory HLA-DR^{HIGH}CD11c^{+} DCs in blood of adeno-associated virus serotype 9 (AAV9)/hucytokines human immune system (HIS) mice upon recombinant adenovirus serotype 5 (rAd5) vaccination. (A) Experimental scheme to generate and vaccinate HIS mice. Eighteen weeks (126 days) post-hematopoietic stem cell (HSC) infusion, HIS mice were vaccinated with AdPfCS and Adp24. One day later, CD11c^{+} DCs were isolated from blood, spleen, and LNs of rAd5-immunized and naive HIS mice, and the level of HLA-DR expression by CD11c^{+} DCs was determined. (B) Two subsets, HLA-DR^{INT} and HLA-DR^{HIGH}, were identified, and their frequency (%) was analyzed by pooled blood or tissue samples from 3 to 5 HIS mice per group, which were given injections containing human HSCs from the same donor. (C) Floating bars that express minimum, maximum, and mean values were overlaid by scatter graphs. The vaccination experiments were repeated twice and results represent 1 experiment (n = 3). Statistical analyses were performed using analysis of variance followed by Dunnett's test, and differences were considered if $P < .05$.

significantly higher CD8^{+} T-cell responses compared with both isolated CD141^{+}CD1c^{-} and CD141^{+}CD1c^{+} DCs, which did not differ in stimulating CD8^{+} T-cell proliferation (Figure 5*C*). These results may indicate that other subsets of mDCs may also contribute to T-cell proliferation.

Because BM-DCs may be an artificial way to test the function of DCs, the proliferation assay was also performed with freshly isolated LN-resident CD11c^{+} DCs from other groups of HIS mice at 12 and 24 hours after AdPfCS/Adp24 immunization. These newly activated LN-resident CD11c^{+} DCs from HIS mice were cocultured with human CD8^{+} T cells collected from HIS mice 15 days after rAd5-immunization as before. Of note, these LN-residing DCs were found to coexpress CD141 and CD1c, indicating their potential in homing in lymphoid organs (Supplementary Figure 2). The freshly isolated human myeloid CD11c^{+} DCs from LNs of malaria/HIV vaccines-immunized HIS mice were able to stimulate malaria/HIV-specific human CD8^{+} T cells in vitro (Figure 5*D*).

Dendritic Cells Coexpressing CD141 and CD1c With Differential MHC-II Expression Expand One Day Postvaccination of Human Immune System Mice

Upregulation of CD141 and CD1c was observed 1 day after vaccination, similar to CD86 within HLA-DR^{+}CD11c^{+} DCs. Therefore, CD141^{+}HLA-DR^{+}CD11c^{+} DCs that also express CD1c were evaluated in detail in blood, spleen, and LNs 0, 1, and 4 days after vaccination with low and high doses of the Ad vaccine (Figure 6*A*). Upregulation of CD1c^{+} within the CD141^{+} DC subset was observed 1 day after rAd5 vaccination, before returning to baseline level by day 4, whereas CD141 continued to rise at day 4 (Figure 6*A* and *B*). The CD1c^{+} subset within CD141^{+} DCs also expressed significantly higher levels of CD86

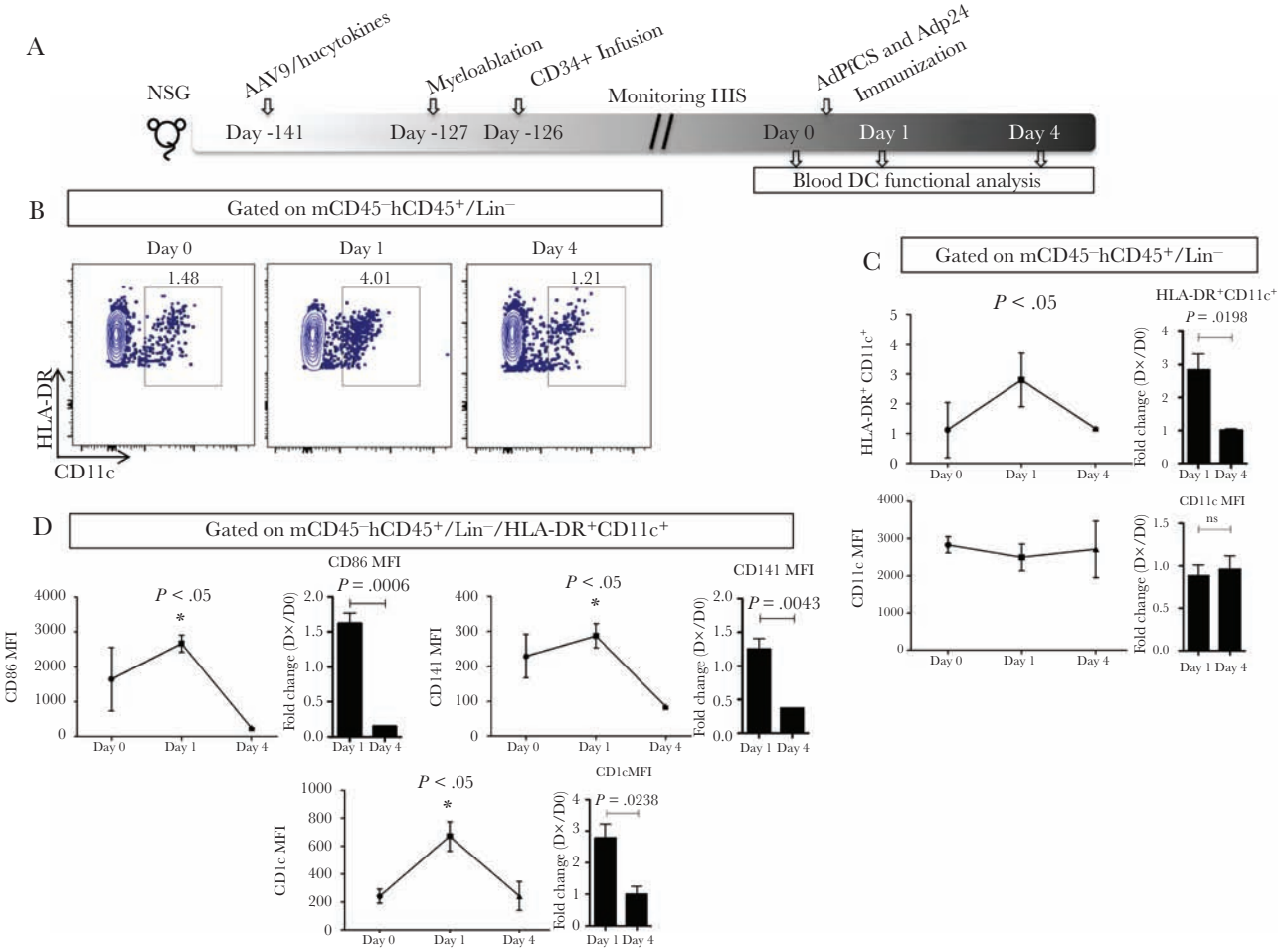

Figure 4. The expansion of human dendritic cells (DCs) in adeno-associated virus serotype 9 (AAV9)/hucytokines human immune system (HIS) mice upon AdPfCS/Adp24 vaccination. (A) Experimental scheme to generate and vaccinate HIS mice. (B) Gating strategy for monitoring myeloid DCs (mDCs) (human leukocyte antigen [HLA]-DR$^+$CD11c$^+$) before (Day 0) and after (Day 1 and 4) AdPfCS/Adp24 vaccination. Cells with the phenotype mCD45$^-$hCD45$^+$/Lin$^-$ were evaluated for the expression of HLA-DR and CD11c on days 0, 1, and 4. Dendritic cells are displayed as density plots. (C) Kinetics of the frequency of HLA-DR$^+$CD11c$^+$ DCs and CD11c expression assessed by geometric mean fluorescence intensity (gMFI) were evaluated within mCD45$^-$hCD45$^+$/Lin$^-$ cells. (D) Expression (gMFI) of phenotypic (CD141 and CD1c) and activation (CD86) molecules within preselected HLA-DR$^+$CD11c$^+$ DCs. Results are displayed as line graphs expressing the mean value and standard error (n = 3). Statistical analyses were performed using analysis of variance followed by Dunnett's test comparing Day 1 and 4 with baseline (Day 0), and differences were considered when $P < .05$. The vaccination experiments were repeated twice and data illustrate 1 representative experiment. NSG, NOD/SCID/IL2Rgamma^{null}.

relative to CD141$^+$CD1c$^-$ DCs regardless of the vaccine dose (Figure 6*C*).

To investigate whether these CD141$^+$CD1c$^+$ DCs had a migratory (DR^{HIGH}) or resident-like (DR^{INT}) profile, CD11c$^+$ DC subsets were evaluated in blood, spleen, and LNs of AAV9/A2$^+$hucytokines HIS mice 1 day after vaccination (Figure 6*D*). The CD141$^+$ DC subset was the most frequent subpopulation in HLA-DR^{HIGH}CD11c$^+$ and HLA-DR^{INT}CD11c$^+$ cells in all tissues tested from HIS mice (Figure 6*E*). It noteworthy to mention that the frequency of double-positive CD141$^+$CD1c$^+$ DCs in LNs was significantly higher than those in spleen and blood only within the migratory HLA-DR^{HIGH} subset (Figure 6*E*). Therefore, double-positive CD141$^+$CD1c$^+$ DCs may have preferential homing capability to the LN after vaccination.

CD141$^+$CD11c$^+$HLA-DR^{HIGH} Dendritic Cells Express Higher Levels of CCR7 in the Lymph Nodes of Human Immune System Mice One Day Postvaccination

As described previously, the transient upregulation of CD1c was observed in the CD141$^+$CD11c$^+$ DC subset 1 day after vaccination and was associated with superior levels of activation. In addition, the frequency of these cells in LNs was higher than in other tissues. Therefore, we evaluated the expression of CD1c and CCR7 among DC subtypes 1 day after vaccination. Vaccination increased the levels of CD1c not only in HLA-DR^{HIGH} but also in HLA-DR^{INT} DC subsets from peripheral blood, spleen, and LNs (Figure 7*A*). CCR7 was selectively increased in HLA-DR^{HIGH}CD11c$^+$ DCs from LNs of vaccinated HIS mice compared to those from naive mice, but no differences were observed in CCR7 expression of HLA-DR^{INT}CD11c$^+$ DCs between vaccinated and naive HIS mice from any tissues (Figure 7*B*). When CCR7 expression between CD1c$^+$

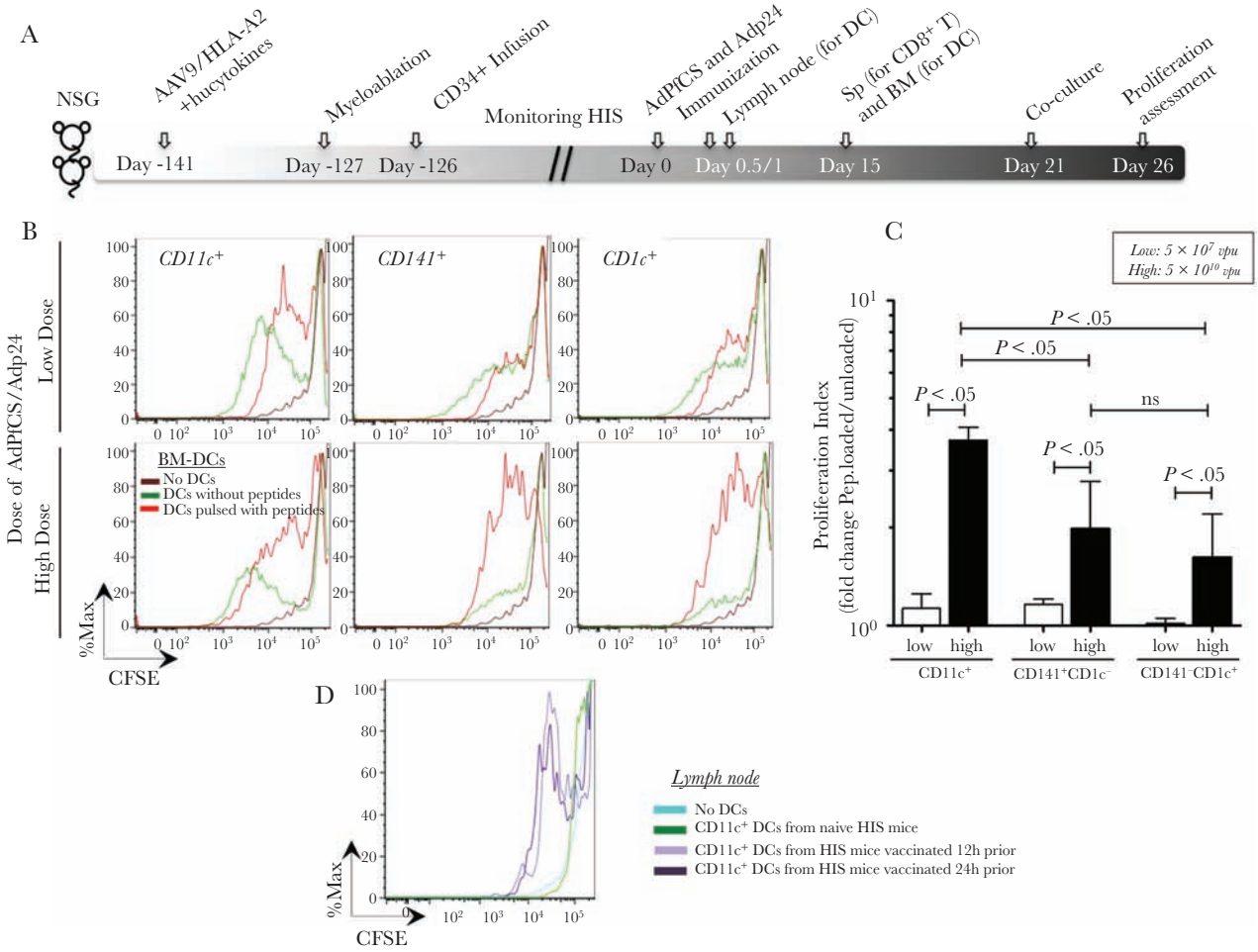

Figure 5. Induction of ex vivo proliferation of antigen-specific $CD8^+$ T cells by human myeloid dendritic cells (DCs) generated in adeno-associated virus serotype 9 (AAV9)-A2/hucytokines human immune system (HIS) mice. (A) Experimental scheme for the generation and vaccination of AAV9-A2/hucytokines HIS mice. Generation of HIS mice was performed as described in Material and Methods. Eighteen weeks (126 days) post-hematopoietic stem cell (HSC) infusion, HIS mice were vaccinated with AdPfCS and Adp24 at low (5×10^7 viral particle units [vpu]) and high (5×10^{10} vpu) doses of each adenovirus. Twelve and 24 hours later, a group of immunized or naive mice (n = 3–5) was sacrificed to collect lymph node (LN)-resident DCs. Fifteen days later, spleen (Sp) and bone marrow (BM) were harvested from another group of recombinant adenovirus serotype 5 (rAd5)-immunized HIS mice (n = 5–7). Bone marrow-DCs were generated and purified to obtain $CD141^+$ and $CD1c^+$ DC subsets, followed by loading with peptides that correspond to $CD8^+$ T-cell epitopes of PfCS protein and p24 antigen. $CD8^+$ T cells were purified from splenocytes and labels with carboxyfluorescein diacetate succinimidyl ester (CFSE). The CFSE-labeled $CD8^+$ T cells and BM-DCs pulsed with or without the peptides were then cocultured for 5 days. (B) The CFSE expression is displayed by fluorescence intensity histograms for $CD8^+$ T cells cocultured with subsets of BM-derived DCs. (C) $CD8^+$ T-cell proliferation indices are shown as bar graphs, which display mean values and standard error (calculated based on the ratio of peptide-loaded versus unloaded DC cultures) for HIS mice immunized with low (white bars) and high (black bars) doses of the rAd5-vaccines. (D) Overlaid histograms display CFSE expression of $CD8^+$ T cells after coculture with $CD11c^+$ DCs that were isolated from LNs of naive HIS mice or immunized HIS mice 12 and 24 hours after vaccination. These experiments were repeated twice, and statistical analyses were performed using analysis of variance followed by Dunnett's test with differences considered if $P < .05$.

and $CD1c^-$ subsets of $CD141^+CD11c^+$ DCs was compared, the $CD1c^+HLA\text{-}DR^{HIGH}$ subset obtained from LNs had the highest expression (Figure 7*C* and *D*). Coexpression of CD141 and CD1c was confirmed by confocal microscopy in LN from HIS mice 1 day after rAd5 vaccination, with both $CD141^+CD1c^-$ DCs and $CD141^+CD1c^+$ DCs observed (Figure 7*E*). These results indicate that different subsets of mDCs were activated in blood and tissues of the HIS mice upon vaccination.

DISCUSSION

The role of human DCs upon vaccination in humanized mouse models have not been thoroughly investigated, particularly with regards to the role of $CD141^+$ and $CD1c^+$ DC subsets in inducing cell-mediated immune responses. Our current study has demonstrated an important role for these DC subsets during vaccination.

In agreement with previous findings [28–32], our results showed that human DCs have a unique phenotypic and distribution pattern in HIS mice and, furthermore, that the phenotypic and distribution pattern of human DCs was quickly altered 1 day after immunization with rAd-based vaccines. Our results have also shown the importance of human GM-CSF and IL-3 in improving the myeloid lineage development, as well as the functionality and maturation of human DCs, as previously

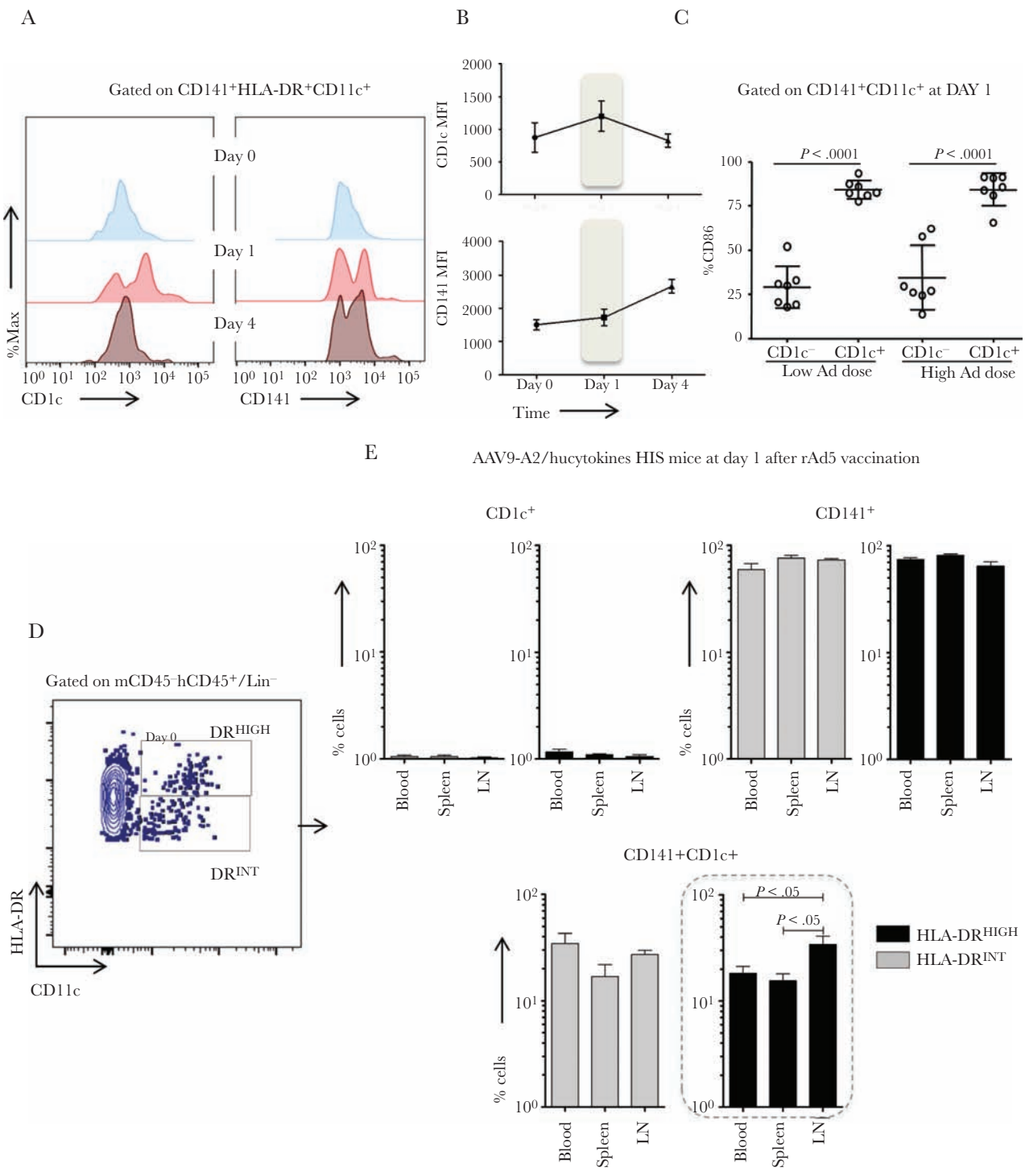

Figure 6. The expansion of human dendritic cells (DCs) that coexpress CD141 and CD1c with differential human leukocyte antigen (HLA)-DR expression in human immune system (HIS) mice 1 day after AdPfCS/Adp24 vaccination. (A and B) Histograms (A) and line graphs (B), respectively, demonstrate the CD1c and CD141 geometric mean fluorescence intensities (MFI) within $CD141^+HLA\text{-}DR^+CD11c^+$ DCs before (Day 0) and after (Day 1 and 4) AdPfCS/Adp24 vaccination. (C) Frequency of $CD141^+HLA\text{-}DR^+CD11c^+$ DCs with or without CD1c expression that are CD86 positive in HIS mice 1 day after low dose versus high dose of AdPfCS/Adp24 vaccination. (D) Gating strategy for identifying $HLA\text{-}DR^{HIGH}$ and $HLA\text{-}DR^{INT}CD11c^+$ DCs (within peripheral lymph/human $CD45^+/Lin^-$ population). (E) Frequency of $CD11c^+$ DC subsets that are single or double positive for CD141 and CD1c in blood, spleen, and lymph node (LN) of HIS mice 1 day after AdPfCS/Adp24 vaccination. Tissue samples, especially LN, were pooled from 7 individual HIS mice that were given injections of human hematopoietic stem cells (HSCs) from the same donor. The results are displayed by bar graphs expressing mean values and standard error (n = 3–7). The dashed line rectangle highlights the significant results for $CD141^+CD1c^+$ DCs. Statistical analyses were performed using analysis of variance followed by Dunnett's test and differences were considered when $P < .05$. The vaccination experiments were repeated twice and data illustrate 1 representative experiment.

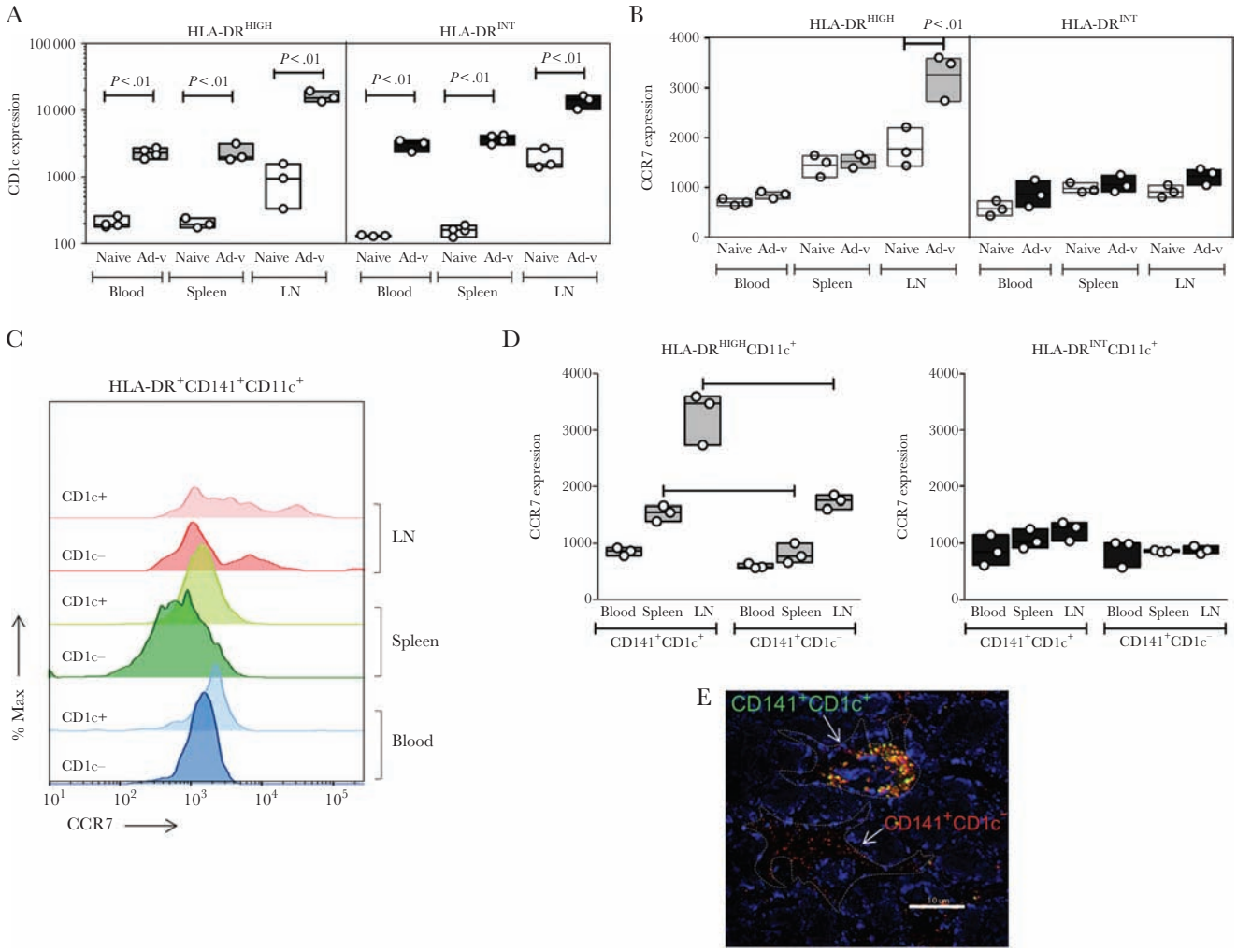

Figure 7. Expression of CCR7 and CD1c in CD141$^+$HLA-DR^{HIGH}CD11c$^+$ dendritic cells (DCs) from blood and tissues of AdPfCS/Adp24-vaccinated human immune system (HIS) mice. CD1c (A) and CCR7 (B) expression in geometric mean fluorescence intensity (gMFI) within HLA-DR^{HIGH} and HLA-DR^{INT}CD11c$^+$ DCs isolated from blood, spleen, and lymph nodes (LNs) of AdPfCS/Adp24-immunized, as well as naive HIS mice. (C) CCR7 expression is displayed in histograms for CD1c$^-$ and CD1c$^+$ subsets within CD141$^+$HLA-DR$^+$CD11c$^+$ DCs isolated from blood, spleen, and LNs of AdPfCS/Adp24-immunized HIS mice. (D) CCR7 expression within HLA-DR^{HIGH} versus HLA-DR^{INT}CD141$^+$CD11c$^+$ DCs with or without CD1c expression. (E) Coexpression of CD141 and CD1c in LN from HIS mice 24 hours after immunization with AdPfCS/Adp24 was assessed by confocal fluorescence microscopy. Lymph nodes were isolated and stained with antihuman CD141 and antihuman CD1c antibodies, and after counterstaining the nuclei with Hoechst 33342, the images were collected using a LSM510 confocal microscope (original magnification, ×100). Dotted lines denote DCs, which are either coexpressing CD141 and CD1c or displaying CD141$^+$CD1c$^-$ phenotype. Tissue samples, especially LN, were pooled from 7 individual HIS mice that were given injections of human hematopoietic stem cells (HSCs) from the same donor. The results are displayed by floating bars expressing minimum, maximum, and mean values overlaid by scatter graphs, which indicate the sample size (n = 3 pools). Statistical analyses were performed using analysis of variance followed by Dunnett's test, and differences were considered when $P < .05$. The vaccination experiments were repeated twice and data illustrate 1 representative experiment.

published [26, 33–36]. It is noteworthy that our AAV9-based gene delivery allows us to deliver an adequate amount of human GM-CSF into NSG mice, thus avoiding the cytokine storm which would be caused by an excessive amount of the cytokine.

CD1c$^+$ DCs have been associated with superior antigen presentation capacity along with robust production of proinflammatory cytokines. A recent report has indicated that CD1c$^+$ DCs have the ability to shape the priming and proliferation of cytotoxic T-cell responses as well as contributing to the maintenance of immune memory [37]. In the context of immunization, CD1c$^+$ DCs were shown to induce tumor-specific immune responses in advanced cancer patients, which clearly demonstrate the applicability of CD1c$^+$ DCs for therapeutic purposes [38]. The present data further expand these findings and show that similar to CD141$^+$ DCs, CD1c$^+$CD11c$^+$ DCs are able to induce proliferation of vaccination-induced CD8$^+$ T cells. In addition, we found an emergence of a double-positive (CD141$^+$CD1c$^+$) DC subset in HIS mice 1 day after immunization with rAd-based vaccines. This subset expresses higher levels of CD86, indicating that they are more activated and prone to engage in costimulation for antigen presentation. CD141$^+$CD1c$^+$ DCs were present in blood, spleen, and draining

LNs of HIS mice. Because CCR7 expressed by DCs is a migratory marker that enables homing of the DCs to the LNs [39, 40], we monitored the expression of this chemokine receptor by DCs in blood and tissues 1 day after vaccination. Upregulation of CCR7 particularly in the $CD141^+CD1c^+$ DC subset was observed when compared with $CD141^+CD1c^-CD11c^+$ DCs, indicating that this DC subset has a higher tendency to migrate to LNs, showing outstanding plasticity in the HIS mouse model [21, 22, 41].

The HLA-DR profile has recently been assessed to define resident ($HLA\text{-}DR^{INT}$) and migratory ($HLA\text{-}DR^{HIGH}$) DCs in human-derived DCs [14]. Therefore, we also determined the level of HLA-DR expression by DCs in our HIS mice upon vaccination with rAd5. We have found that rAd5 vaccination increased the $HLA\text{-}DR^{INT}CD11c^+$ DC subset in LNs and spleen and $HLA\text{-}DR^{HIGH}CD11c^+$ DCs in blood of the HIS mice. Our results are corroborated by the findings that a combination therapy of the adoptive transfer of DCs pulsed with Wilms Tumor-1 peptide and chemotherapy increased the level of HLA-DR expression on circulating DCs from patients with pancreatic cancer [42, 43].

CONCLUSIONS

These data, taken together, suggest that the transient but significant upregulation of CD1c is a result of $CD141^+$ DC activation upon vaccination in our HIS mice. In addition, the results presented herein shed some light in regard to CD141 and CD1c expression within human $CD11c^+$ DC subsets during vaccination, which could be a potential target for future adjuvant development in the context of various vaccine platforms in humans.

Supplementary Data

Supplementary materials are available at The *Journal of Infectious Diseases* online. Consisting of data provided by the authors to benefit the reader, the posted materials are not copyedited and are the sole responsibility of the authors, so questions or comments should be addressed to the corresponding author.

Supplementary Figure 1. Human leukocyte antigen (HLA)-A2 expression, as opposed to hematopoietic cytokines, does not significantly improve the reconstitution of human plasmacytoid dendritic cells (pDCs) and myeloid DCs (mDCs) in NOD/SCID/IL2Rgamma^{null} (NSG) mice after hematopoietic stem cells (HSCs) infusion. The NSG mice were treated with recombinant adeno-associated virus serotype 9 (rAAV9) encoding HLA-A2 only (n = 6) or a mixture of rAAV9 encoding HLA-A2, interleukin (IL)-3, IL-15, and granulocyte-macrophage colony-stimulating factor (GM-CSF). Plasmacytoid DCs ($CD304^+CD123^+$) and mDCs ($CD1c^+CD11c^+$; $CD141^+CD11c^+$) were monitored by flow cytometry 14 weeks after HSC infusion and absolute DC numbers (left), and percentage of human DCs (right) among $CD45^+$ cells are represented as floating bars overlaid with scatter plots for rAAV9/HLA-A2-treated NSG mice (Δ) or rAAV9/HLA-A2/hucytokines-treated NSG mice (○). Dendritic cell absolute numbers are expressed within 5×10^5 mononuclear (MN) cells obtained from peripheral blood. Statistical analyses were performed using analysis of variance followed by Dunnett's test, and differences were considered when $P < .05$. Results between the 2 groups of mice were not significant ($P > .05$).

Supplementary Figure 2. Immunohistofluorescence assay was performed on lymph nodes (LNs) collected from human immune system (HIS) mice 24 hours after immunization with AdPfCS/Adp24. The LNs were isolated and stained with antihuman CD141 and antihuman CD1c antibodies, and after counterstaining the nuclei with Hoechst 33342, the images were collected using a LSM510 confocal microscope (original magnification, ×100).

Notes

Acknowledgments. We thank Vincent Sahi for technical assistance with flow cytometry. We also thank the late Ruth Nussenzweig (in memoriam) for insightful comments and incentive in the beginning of this study.

Financial support. This work was funded by a grant from the National Institutes of Health (AI070258; to M. T.). J. G. A. C.-d.-R. received a fellowship from the Irene Diamond Fund (Aaron Diamond AIDS Research Center) and Brazilian National Program for Postdoctoral Training given by Coordenação de Aperfeiçoamento de Pessoal de Nível Superior (CAPES/PNPD-Brazil).

Potential conflicts of interest. All authors: No reported conflicts of interest. All authors have submitted the ICMJE Form for Disclosure of Potential Conflicts of Interest.

References

1. Steinman RM, Cohn ZA. Identification of a novel cell type in peripheral lymphoid organs of mice. I. Morphology, quantitation, tissue distribution. J Exp Med **1973**; 137:1142–62.
2. Banchereau J, Steinman RM. Dendritic cells and the control of immunity. Nature **1998**; 392:245–52.
3. Helft J, Ginhoux F, Bogunovic M, Merad M. Origin and functional heterogeneity of non-lymphoid tissue dendritic cells in mice. Immunol Rev **2010**; 234:55–75.
4. Guilliams M, Ginhoux F, Jakubzick C, et al. Dendritic cells, monocytes and macrophages: a unified nomenclature based on ontogeny. Nat Rev Immunol **2014**; 14:571–8.
5. Naik SH, Sathe P, Park HY, et al. Development of plasmacytoid and conventional dendritic cell subtypes from single precursor cells derived in vitro and in vivo. Nat Immunol **2007**; 8:1217–26.
6. Liu K, Victora GD, Schwickert TA, et al. In vivo analysis of dendritic cell development and homeostasis. Science **2009**; 324:392–7.
7. Dzionek A, Fuchs A, Schmidt P, et al. BDCA-2, BDCA-3, and BDCA-4: three markers for distinct subsets of

dendritic cells in human peripheral blood. J Immunol **2000**; 165:6037–46.
8. MacDonald KP, Munster DJ, Clark GJ, Dzionek A, Schmitz J, Hart DN. Characterization of human blood dendritic cell subsets. Blood **2002**; 100:4512–20.
9. Haniffa M, Shin A, Bigley V, et al. Human tissues contain CD141hi cross-presenting dendritic cells with functional homology to mouse CD103+ nonlymphoid dendritic cells. Immunity **2012**; 37:60–73.
10. Meixlsperger S, Leung CS, Rämer PC, et al. CD141+ dendritic cells produce prominent amounts of IFN-α after dsRNA recognition and can be targeted via DEC-205 in humanized mice. Blood **2013**; 121:5034–44.
11. Bachem A, Güttler S, Hartung E, et al. Superior antigen cross-presentation and XCR1 expression define human CD11c+CD141+ cells as homologues of mouse CD8+ dendritic cells. J Exp Med **2010**; 207:1273–81.
12. Traver D, Akashi K, Manz M, et al. Development of CD8alpha-positive dendritic cells from a common myeloid progenitor. Science **2000**; 290:2152–4.
13. Shortman K, Heath WR. The CD8+ dendritic cell subset. Immunol Rev **2010**; 234:18–31.
14. Esterházy D, Loschko J, London M, Jove V, Oliveira TY, Mucida D. Classical dendritic cells are required for dietary antigen-mediated induction of peripheral T(reg) cells and tolerance. Nat Immunol **2016**; 17:545–55.
15. Bedoui S, Whitney PG, Waithman J, et al. Cross-presentation of viral and self antigens by skin-derived CD103+ dendritic cells. Nat Immunol **2009**; 10:488–95.
16. Lundie RJ, de Koning-Ward TF, Davey GM, et al. Blood-stage *Plasmodium* infection induces CD8+ T lymphocytes to parasite-expressed antigens, largely regulated by CD8alpha+ dendritic cells. Proc Natl Acad Sci U S A **2008**; 105:14509–14.
17. Belz GT, Bedoui S, Kupresanin F, Carbone FR, Heath WR. Minimal activation of memory CD8+ T cell by tissue-derived dendritic cells favors the stimulation of naive CD8+ T cells. Nat Immunol **2007**; 8:1060–6.
18. Shultz LD, Brehm MA, Garcia-Martinez JV, Greiner DL. Humanized mice for immune system investigation: progress, promise and challenges. Nat Rev Immunol **2012**; 12:786–98.
19. Li Y, Mention JJ, Court N, et al. A novel Flt3-deficient HIS mouse model with selective enhancement of human DC development. Eur J Immunol **2016**; 46:1291–9.
20. Chen P, Huang Y, Womer KL. Effects of mesenchymal stromal cells on human myeloid dendritic cell differentiation and maturation in a humanized mouse model. J Immunol Methods **2015**; 427:100–4.
21. Yu CI, Becker C, Wang Y, et al. Human CD1c+ dendritic cells drive the differentiation of CD103+ CD8+ mucosal effector T cells via the cytokine TGF-β. Immunity **2013**; 38:818–30.
22. Yu CI, Becker C, Metang P, et al. Human CD141+ dendritic cells induce CD4+ T cells to produce type 2 cytokines. J Immunol **2014**; 193:4335–43.
23. Saito Y, Ellegast JM, Manz MG. Generation of humanized mice for analysis of human dendritic cells. Methods Mol Biol **2016**; 1423:309–20.
24. Flotte TR, Carter BJ. Adeno-associated virus vectors for gene therapy. Gene Ther **1995**; 2:357–62.
25. Zincarelli C, Soltys S, Rengo G, Rabinowitz JE. Analysis of AAV serotypes 1-9 mediated gene expression and tropism in mice after systemic injection. Mol Ther **2008**; 16:1073–80.
26. Huang J, Li X, Coelho-dos-Reis JG, Wilson JM, Tsuji M. An AAV vector-mediated gene delivery approach facilitates reconstitution of functional human CD8+ T cells in mice. PLoS One **2014**; 9:e88205.
27. Huang J, Li X, Coelho-dos-Reis JG, et al. Human immune system mice immunized with *Plasmodium falciparum* circumsporozoite protein induce protective human humoral immunity against malaria. J Immunol Methods **2015**; 427:42–50.
28. Palucka AK, Gatlin J, Blanck JP, et al. Human dendritic cell subsets in NOD/SCID mice engrafted with CD34+ hematopoietic progenitors. Blood **2013**; 102:3302–10.
29. Ding Y, Wilkinson A, Idris A, et al. FLT3-ligand treatment of humanized mice results in the generation of large numbers of CD141+ and CD1c+ dendritic cells in vivo. J Immunol **2014**; 192:1982–9.
30. Vuckovic S, Abdul Wahid FS, Rice A, et al. Compartmentalization of allogeneic T-cell responses in the bone marrow and spleen of humanized NOD/SCID mice containing activated human resident myeloid dendritic cells. Exp Hematol **2008**; 36:1496–506.
31. Kodama A, Tanaka R, Saito M, Ansari AA, Tanaka Y. A novel and simple method for generation of human dendritic cells from unfractionated peripheral blood mononuclear cells within 2 days: its application for induction of HIV-1-reactive CD4(+) T cells in the hu-PBL SCID mice. Front Microbiol **2013**; 4:292.
32. Harui A, Kiertscher SM, Roth MD. Reconstitution of huPBL-NSG mice with donor-matched dendritic cells enables antigen-specific T-cell activation. J Neuroimmune Pharmacol **2011**; 6:148–57.
33. Zhan Y, Carrington EM, van Nieuwenhuijze A, et al. GM-CSF increases cross-presentation and CD103 expression by mouse $CD8^+$ spleen dendritic cells. Eur J Immunol **2011**; 41:2585–95.
34. Greter M, Helft J, Chow A, et al. GM-CSF controls nonlymphoid tissue dendritic cell homeostasis but is

dispensable for the differentiation of inflammatory dendritic cells. Immunity **2012**; 36:1031–46.
35. Edelson BT, Bradstreet TR, KC W, et al. Batf3-dependent CD11b(low/-) peripheral dendritic cells are GM-CSF-independent and are not required for Th cell priming after subcutaneous immunization. PLoS One **2011**; 6:e25660.
36. Kashiwada M, Pham NL, Pewe LL, Harty JT, Rothman PB. NFIL3/E4BP4 is a key transcription factor for CD8α$^+$ dendritic cell development. Blood **2011**; 117:6193–7.
37. Nizzoli G, Larghi P, Paroni M, et al. IL-10 promotes homeostatic proliferation of human CD8(+) memory T cells and, when produced by CD1c(+) DCs, shapes naive CD8(+) T-cell priming. Eur J Immunol **2016**; 46:1622–32.
38. Schreibelt G, Bol KF, Westdorp H, et al. Effective clinical responses in metastatic melanoma patients after vaccination with primary myeloid dendritic cells. Clin Cancer Res **2016**; 22:2155–66.
39. Förster R, Davalos-Misslitz AC, Rot A. CCR7 and its ligands: balancing immunity and tolerance. Nat Rev Immunol **2008**; 8:362–71.
40. Ohl L, Mohaupt M, Czeloth N, et al. CCR7 governs skin dendritic cell migration under inflammatory and steady-state conditions. Immunity **2004**; 21:279–88.
41. Jung KC, Park CG, Jeon YK, et al. In situ induction of dendritic cell-based T cell tolerance in humanized mice and nonhuman primates. J Exp Med **2011**; 208:2477–88.
42. Takakura K, Koido S, Kan S, et al. Prognostic markers for patient outcome following vaccination with multiple MHC class I/II-restricted WT1 peptide-pulsed dendritic cells plus chemotherapy for pancreatic cancer. Anticancer Res **2015**; 35:555–62.
43. Koido S, Homma S, Okamoto M, et al. Treatment with chemotherapy and dendritic cells pulsed with multiple Wilms' tumor 1 (WT1)-specific MHC class I/II-restricted epitopes for pancreatic cancer. Clin Cancer Res **2014**; 20:4228–39.